East European Journal of Physics. **3**. 432–442 (2026)
DOI: 10.26565/2312-4334-2026-3-39 ISSN 2312-4334

THE INFLUENCE OF JOULE HEATING EFFECT AND THERMAL STRATIFICATION ON MHD TERNARY HYBRID NANOFLUID IN A POROUS MEDIUM OVER A VERTICALLY STRETCHING CYLINDER: A NUMERICAL INVESTIGATION

Surajit Dutta[1], **Nitul Kalita**[2], **Rupam Shankar Nath**[3*], **Rudra Kanta Deka**[2]
[1]*Department of Mathematics, C.N.B. College, Bokakhat-785612, Assam, India*
[2]*Department of Mathematics, Gauhati University, Guwahati-781014, Assam, India*
[3]*Department of Mathematics, Morigaon College (Autonomous), Morigaon-782105, Assam, India*
[*]*Corresponding Author e-mail: rupamnath23@gmail.com*
Received May 28, 2026; revised July 6, 2026; accepted July 21, 2026

The aspects of flow in a magnetohydrodynamic (MHD) ternary hybrid nanofluid consisting of suspended (Cu), aluminum oxide (Al_2O_3), and titanium dioxide (TiO_2) nanoparticles in water (H_2O) were numerically investigated in this study. The effects of thermal stratification and Joule heating are incorporated by passing the nanofluid through a vertically extending cylinder in a porous medium. By implementing an appropriate transformation, the energy and boundary layer equations are simplified to a nonlinear ODE system. The resulting system is solved using MATLAB's fourth-order accurate bvp4c solver. from MATLAB is employed to solve the altered system. The effects are illustrated graphically the change in velocity and temperature and quantitatively tabulate the changes in friction factor, and heat transfer rate for important values of the dimensionless physical factors related to the problem. Crucial findings show that, hybrid nanofluids outperform nanofluids in terms of thermal conductivity. Temperature and velocity of the ternary hybrid nanofluid are both decreased when the heat stratification factor is present, as compared to the absence of stratification. There is a noticeable increase in the heat transfer rate when the ternary hybrid nanofluid is compared with the hybrid nanofluid, which in turn surpasses that of traditional nanofluids. The acquired results are valuable for applications in geothermal energy extraction, chemical processing, and materials synthesis.

Keywords: *Ternary Hybrid Nanofluid; Joule's Effect; Stretching Vertical Cylinder; Thermal Stratification; Porous Medium; bvp4c*

1. INTRODUCTION

Ternary hybrid nanofluids are a state-of-the-art breakthrough in fluid dynamics and nanotechnology that have broad engineering applications in engineering and industries. There are three different kinds of nanoparticles mixed in with a base fluid to make these nanofluids. These fluids possess enhanced thermal and rheological properties. The nanoparticles can be metallic or non-metallic, and the base fluid can be any common heat transfer fluid or coolant such water, ethylene glycol, or oil. This article describes a research investigation on a ternary hybrid nanofluid consisting of copper (Cu), aluminum oxide (Al_2O_3), and titanium dioxide (TiO_2) nanoparticles. The nanoparticles are uniformly dispersed inside a fluid medium containing water.

Research has shown that adding copper (Cu) nanoparticles to a nanofluid improves its thermal conductivity, while adding aluminum oxide (Al_2O_3) and titanium dioxide (TiO_2) nanoparticles improves the efficiency and stability of heat transmission. In order to improve thermal management and heat dissipation, this nanofluid can be used in a variety of applications, including cooling systems, electrical devices, and heat exchangers. It is well-known that copper nanoparticles can kill bacteria, and (TiO_2) nanoparticles can fight bacteria and other microbes by photo catalysis. Nanoparticles of titanium dioxide (TiO_2) with photocatalytic characteristics can help decompose organic pollutants and purify water. The ternary hybrid nanofluid comprising Cu, Al_2O_3 and TiO_2 could be useful in water treatment processes, removing contaminants and improving water quality in the process.

An innovative new class of fluids called nanofluids was created by mixing a base fluid with particles as small as a few nanometers in size. These tiny particles, which might be metallic or non-metallic, are usually less than 100 nanometers. A novel class of heat transfer fluids including free-floating metallic nanoparticles has been proposed by the idea of nanofluid, which was initially introduced by Choi and Eastman [1]. Several researchers have investigated a sliding vertical plate in Das and Jana [2] and a vertical channel in Das et al. [3] in relation to the radiation-induced natural convective flow of nanofluids. In their respective studies, Reddy et al.[4] and Mahanthesh et al. [5] assessed the consequences of mass and heat transfer on nanofluid as it traverses a mobile or static vertical plate, while considering the impact of a chemical reactions and a heat source. In their study, Sandeep and Reddy [6] investigated the flow of a magnetohydrodynamic (MHD) Cu-water nanofluid over a cone and a wedge, considering the influence of nonlinear thermal radiation. Moreover, the Lattice Boltzmann approach was utilized in the investigation of the magnetohydrodynamic (MHD) Cu-water nanofluid, given the influence of Lorentz forces by Sheikholeslami et al., [7]. The investigation conducted by Rashidi et al. [8] proposed a Lie group solution for the issue of the production or consumption of heat in the context of nanofluid movement over a horizontal plate undergoing chemical reactions. The HAM is employed in Abolbashari et al. [9] to examine the entropy of a nanofluid

Cite as: S. Dutta, N. Kalita, R. S. Nath, R. K. Deka, East Eur. J. Phys. 3, 432 (2026), https://doi.org/10.26565/2312-4334-2026-3-39

comprising water as the main fluid and one of four different types of nanoparticles: TiO_2, Al_2O_3, Cu, and CuO. The nanofluid flows through a stretchy permeable surface. Within the framework of velocity slip and heat leap, an analytical study was conducted by Turkyilmazoglu [10] to examine the MHD nanofluid flow of different water-soluble nanoparticles as they flowing over a periodically stretching and shrinking permeable sheet. The impacts of heat radiation, heat diffusion, and viscous dissipation were investigated numerically in a study of nanofluid boundary layer flow across a moving flat plate by Motsumi and Makinde [11]. Nath and Deka [12], Kalita et al., [13] and Nath et al. [14] studied how temperature layering and chemical reactions affect the flow across infinite and accelerated vertical plates, respectively. Cheng [15, 16] investigated the effects of mass and heat stratification across a wavy surface and a vertical, truncated cone, respectively. In addition, for infinite vertical cylinders, Paul and Deka [17] have studied the effects of both stratification factors. [18] Considered the impacts of mass and temperature layering on the unstable flow through an endlessly fast-moving upright plate in a porous media with exponential mass diffusion and fluctuating temperatures. The unstable parabolic flow across an infinite upright plate in a porous media with varying mass diffusion and an exponentially decreasing temperature was studied by [19] in relation to the unite effects of temperature and mass stratification. Using a vertically expanding cylinder in porous medium, Nath and Deka [20] studied how the flow of water-based hybrid, nano, and ternary hybrid nanofluids via magnetohydrodynamics (MHD) is impacted by temperature stratification. The study in Paul et al. [18] examines the impact of temperature stratification on a hybrid nanofluid composed of $Cu - Al_2O_3/H_2O$ in a porous media. The research conducted by the authors focused on a cylinder that is stretched vertically, and examines the impact of a heat sink or source. It was observed that the thermal conductivity of hybrid nanofluids exhibited a notable increase in comparison to that of nanofluids. Thus, the application of hybrid nanofluids demonstrates a substantial impact on improving thermal improvements. The study conducted by Rana and Kumar [19] inspected the flow of hybrid nano liquid via a rotating cylinder, considering the influence of quadratic heat radiation on a buoyancy-driven nonlinear flow. To enhance the ternary hybrid nanofluid's $Cu - Al_2O_3 - MWCNT$/water heat conveyance capabilities consisting of, the researchers in reference Shanmugapriya et al., [20] examined the impact of nanoparticle morphology. In their study, Shaik et al. [21] looked into the free convection that happens in a wavy, sinusoidal shell that contains a hybrid nanofluid made of $TiO_2 - Cu$ particles that are suspended in water. The consequences of thermal radiation, internal heat creation, a magnetic field with an angle on convection is included in the analysis. Examining the responses of the similar formulas that govern the behavior of a colloidal combination of water, cylindrical grapheme, round nanotubes of carbon, and platelet nanoparticles made of alumina was done by Cao et al., [22]. In addition, the study examined forced, free, and mixed convection regimes, the study took into account different degrees of partial slide. Research on the heat transfer properties of ternary hybrid nanofluid flows in the existence of nonlinear heat radiation and a magnetized dipole was carried out by Nasir et al. [23]. Using a convectively heated stretching/shrinking cylinder, the effects of suction and heat source on the MHD stagnation point flow of a ternary hybrid nanofluid ($Cu - Fe_3O_4 - SiO_2$/polymer) have been studied by Mahmood et al. [24]. Furthermore, in the framework of electromagnetic hydrodynamics (EMHD), a ternary hybrid nanofluid consisting of $Cu - CNT - Ti$ and water was studied by Jakeer et al. [25] to determine the effects of non-linear Darcy-Forchheimer flow. Compared to nanofluid or hybrid nanofluid alone, the ternary hybrid nanofluid significantly affected the temperature profile. Patil et al. [26] Look at how a ternary hybrid nanofluid ($THNF$) flows with tangent hyperbolic ($(T-H)$) flow features when it meets a rough-yawed cylinder. Impulsive forces are used to move the cylinder, and the study is mostly about the mixed convection process and periodic magnetohydrodynamics. Gorfie et al. [27] addressed the combined effects of Joule heating and thermal stratification on MHD ternary hybrid nanofluid flow over a vertically stretching cylinder embedded in a porous medium remain limited, thereby motivating the present investigation. Kumar et al. [28] studied on stretching-cylinder flows have shown that Joule heating, magnetic fields, and internal heat generation significantly affect the velocity and temperature distributions of electrically conducting fluids. Motivated by these findings, the present work extends the analysis to an MHD ternary hybrid nanofluid in a porous medium by incorporating the combined effects of Joule heating and thermal stratification over a vertically stretching cylinder.

As shown in the literature review, previous research has not attempted to demonstrate the flow of a magnetohydrodynamic (MHD) ternary nanofluid via a vertically expanding cylinder in a porous medium, taking into account the influence of the joule's impact and temperature stratification effect. Examining the heat transfer characteristics of a ternary hybrid nanofluid made up of $Cu - Al_2O_3 - TiO_2$ particles distributed in water is the core objective of this work. This study examines the behavior of heat transport around a vertically stretching cylinder while taking into the account of homogeneous thermal sources and thermal sinks, the joule's effect, and thermal stratification. By employing suitable self-similar variables within the bvp4c solver of the MATLAB programmed, the non-linear partial differential equations (PDEs) that govern the flow are changed into ordinary differential equations (ODEs). As shown by its description and application in MATLAB by [30], and Hale and Moore [29], the Bvp4c technique is well-known and used to simulate the problem in this study. For various parameters like $\lambda, \delta, Pr, M, Q$ and Ec the results are presented graphically.

2. METHODOLOGY

In the context of a vertical stretchable cylinder with radius r_0, let us contemplate a two-dimensional steady incompressible ternary hybrid nanofluid composed of $Cu - Al_2O_3 - TiO_2/H_2O$. This nanofluid is submerged in a porous medium. Thermal stratification, a heat source/sink, and joule's effect exert an influence on the system. As displayed in Fig. 1, it is postulated that the ternary hybrid nanofluid flows in the axial x-direction, where the r coordinate denotes the

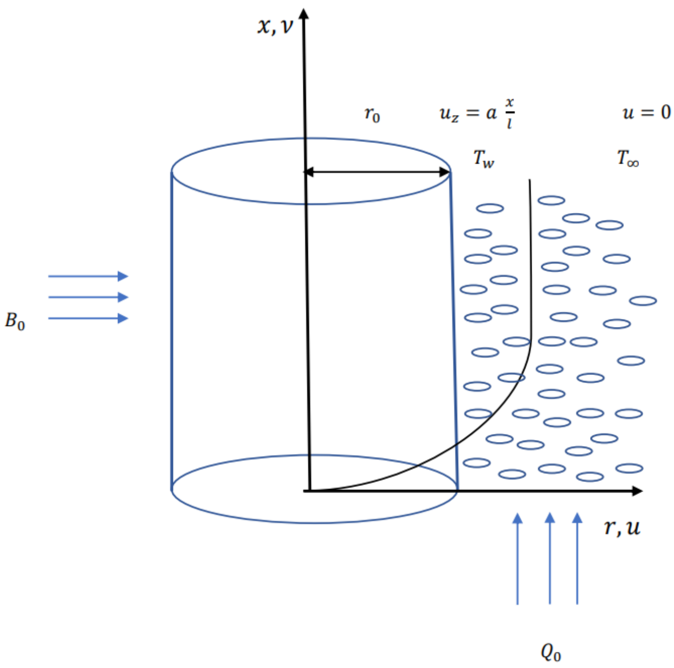

Figure 1. Physical Model and Coordinate system

direction perpendicular to the x-axis. Here, "u" stands for the ternary hybrid nanofluid's velocity component along the r-axis and "v" for the x-axis. In the present investigation, a magnetic field of magnitude B_0 is supplied perpendicular to the ternary hybrid nanofluid's propagation path. In addition to Joule heating, the thermal buoyancy effect is taken into account in the flow problem. $u = a\frac{x}{l}$, is the velocity responsible for inducing linear stretching in the upright cylinder, where $'a'$ and $'l'$ symbolise the cylinder's characteristic length and velocity, respectively. $T_w(x) = T_0 + A\left(\frac{x}{l}\right)$, is the wall's assumed temperature, and $T_\infty(x) = T_0 + B\left(\frac{x}{l}\right)$, is the ternary hybrid nanofluid's temperature at ambient conditions. The constants T_0 and A, B stand for the beginning temperature and non-negative constants, respectively. According to the study conducted by Paul et al., [18], the equations that regulate continuity, momentum, and energy in the setting of a ternary hybrid nanofluid can be formulated as follows.

$$\frac{\partial(ru)}{\partial x} + \frac{\partial(rv)}{\partial r} = 0 \tag{1}$$

$$u\frac{\partial u}{\partial x} + v\frac{\partial u}{\partial r} = \frac{\mu_{thnf}}{\rho_{thnf}}\frac{1}{r}\frac{\partial}{\partial r}\left(r\frac{\partial u}{\partial r}\right) + \frac{(\rho\beta_T)_{thnf}}{\rho_{thnf}}g(T - T_\infty) - \frac{\sigma_{thnf}}{\rho_{thnf}}B_0^2 u - \frac{\mu_{thnf}}{\rho_{thnf}}\frac{u}{k'} \tag{2}$$

$$u\frac{\partial T}{\partial x} + v\frac{\partial T}{\partial r} = \frac{k_{thnf}}{(\rho c_p)_{thnf}}\frac{1}{r}\frac{\partial}{\partial r}\left(r\frac{\partial T}{\partial r}\right) + \frac{Q_0}{(\rho c_p)_{thnf}}(T - T_\infty) + \frac{\sigma_{thnf}}{(\rho c_p)_{thnf}}B_0^2 u^2 \tag{3}$$

The boundary conditions are as follows:

$$u = a\frac{x}{l}, \quad v = 0, \quad T = T_w(x) \quad \text{when } r = r_0$$

$$u = 0, \quad T \to T_\infty(x) \quad \text{when } r \to \infty$$

Here is the similarity transformation utilized in Equations (1)-(3), as described in reference [18]

$$\eta = \frac{r^2 - r_0^2}{2r_0}\sqrt{\frac{a}{\nu_f l}}, \quad \psi = \sqrt{\frac{a\nu_f}{l}}xr_0 f(\eta), \quad \theta = \frac{T - T_\infty(x)}{T_w(x) - T_0}$$

and we have the following non-dimensional quantities:

$$M = \frac{l\sigma_f B_0^2}{a\rho_f}, \quad K = \frac{l\nu_f}{ak}, \quad \gamma = \sqrt{\frac{l\nu_f}{ar_0^2}}, \quad \lambda = \frac{Gr}{Re_x^2}, \quad \delta = \frac{B}{A}, \quad Q = \frac{Q_0 l}{a(\rho c_p)_f},$$

$$Pr = \frac{\nu_f(\mu c_p)_f}{k_f}, \quad Ec = \frac{u_z^2}{(c_p)_f(T_w(x) - T_0)}$$

In this context, K denotes the porosity parameter, γ signifies the curvature parameter, M represents the magnetic parameter, λ signifies the thermal buoyancy parameter, Q signifies the heat source/sink parameter, Pr represents the Prandtl number, δ signifies the thermal stratification parameter, and Ec represents the Eckert number.

To satisfy equation (1) for continuity, we introduce the stream function ψ, which has the form $u = \frac{1}{r}\frac{\partial\psi}{\partial r}$ and $v = -\frac{1}{r}\frac{\partial\psi}{\partial x}$. Thus, we provide the non-dimensional representations of the altered equations as follows:

$$f'^2 - ff'' = a_1\left[2\gamma f'' + (1 + 2\gamma\eta)f'''\right] + a_2\lambda\theta - (a_3 M + a_1 K)f' \tag{4}$$

$$f'(\theta + \delta) - f\theta' = a_4\left[2\gamma\theta' + (1 + 2\gamma\eta)\theta''\right] + a_5\theta + a_6 EcMf'^2 \tag{5}$$

where,

$$x_1 = \frac{\mu_{thnf}}{\mu_f}, \quad x_2 = \frac{\rho_f}{\rho_{thnf}}, \quad x_3 = \frac{(\rho\beta)_{thnf}}{(\rho\beta)_f}, \quad x_4 = \frac{(\rho C_p)_f}{(\rho C_p)_{thnf}}, \quad x_5 = \frac{\sigma_{thnf}}{\sigma_f}, \quad x_6 = \frac{k_{thnf}}{k_f}$$

$$a_1 = x_1 x_2, \quad a_2 = x_2 x_3, \quad a_3 = x_2 x_5, \quad a_4 = \frac{x_4 x_6}{Pr}, \quad a_5 = Qx_4, \quad a_6 = x_4 x_5$$

The symbols $\mu_{thnf}, \rho_{thnf}, (\beta)_{thnf}, (\rho C_p)_{thnf}, \sigma_{thnf}, k_{thnf}$ indicate the ternary hybrid nanofluid's coefficient of viscosity, electrical conductivity, thermal expansion, heat capacity, density and thermal conductivity, respectively. Additionally, $\mu_f, \rho_f, (\beta)_f, (\rho C_p)_f, \sigma_f, k_f$ represent the viscosity, electrical conductivity, thermal expansion, heat capacity, density, and thermal conductivity of the base fluid, respectively.

The dimensionless coefficients $a_1 - a_6$ appearing in Eqs. (4) and (5) are introduced to simplify the transformed governing equations. These coefficients represent the effective thermo-physical property ratios of the ternary hybrid nanofluid relative to the base fluid and account for the combined effects of viscosity, density, thermal expansion, electrical conductivity, heat capacity, thermal conductivity, heat source, and Joule heating.

The transformed boundary conditions are as follows:

$$\begin{array}{llll} f(\eta) = 0 & f'(\eta) = 1 & \theta(\eta) = 1 - \delta & \text{at } \eta = 0 \\ & f'(\eta) \to 0 & \theta(\eta) \to 0 & \text{as } \eta \to \infty \end{array} \tag{6}$$

The ternary hybrid nanofluid has the following thermo-physical properties [25] :

$$\mu_{thnf} = \frac{\mu_f}{(1-\phi_1)^{2.5}(1-\phi_2)^{2.5}(1-\phi_3)^{2.5}}$$

$$\rho_{thnf} = (1-\phi_3)\left[(1-\phi_2)\left\{(1-\phi_1)\rho_f + \phi_1\rho_{s1}\right\} + \phi_2\rho_{s2}\right] + \phi_3\rho_{s3}$$

$$(\rho c_p)_{thnf} = (1-\phi_3)\left[(1-\phi_2)\left\{(1-\phi_1)(\rho c_p)_f + \phi_1(\rho c_p)_{s1}\right\} + \phi_2(\rho c_p)_{s2}\right] + \phi_3(\rho c_p)_{s3}$$

$$(\rho\beta_T)_{thnf} = (1-\phi_3)\left[(1-\phi_2)\left\{(1-\phi_1)(\rho\beta_T)_f + \phi_1(\rho\beta_T)_{s1}\right\} + \phi_2(\rho\beta_T)_{s2}\right] + \phi_3(\rho\beta_T)_{s3}$$

$$k_{nf} = \left[\frac{(k_{s1} + 2k_f) - 2\phi_1(k_f - k_{s1})}{(k_{s1} + 2k_f) + \phi_1(k_f - k_{s1})}\right]k_f, \; k_{hnf} = \left[\frac{(k_{s2} + 2k_{nf}) - 2\phi_2(k_{nf} - k_{s2})}{(k_{s2} + 2k_{nf}) + \phi_2(k_{nf} - k_{s2})}\right]k_{nf}$$

$$k_{thnf} = \left[\frac{(k_{s3} + 2k_{hnf}) - 2\phi_3(k_{hnf} - k_{s3})}{(k_{s3} + 2k_{hnf}) + \phi_3(k_{hnf} - k_{s3})}\right]k_{hnf}, \; \sigma_{nf} = \left[\frac{(\sigma_{s1} + 2\sigma_f) - 2\phi_1(\sigma_f - k_{s1})}{(\sigma_{s1} + 2\sigma_f) + \phi_1(\sigma_f - \sigma_{s1})}\right]\sigma_f$$

$$\sigma_{hnf} = \left[\frac{(\sigma_{s2} + 2\sigma_{nf}) - 2\phi_2(\sigma_{nf} - \sigma_{s2})}{(\sigma_{s2} + 2\sigma_{nf}) + \phi_2(\sigma_{nf} - \sigma_{s2})}\right]\sigma_{nf}, \sigma_{thnf} = \left[\frac{(\sigma_{s3} + 2\sigma_{hnf}) - 2\phi_3(\sigma_{hnf} - \sigma_{s3})}{(\sigma_{s3} + 2\sigma_{hnf}) + \phi_3(\sigma_{hnf} - \sigma_{s3})}\right]\sigma_{hnf}$$

where ϕ_1, ϕ_2 and ϕ_3 are volume fraction of Cu(Copper), Al_2O_3 (aluminium oxide) and TiO_2(titanium oxide) nanoparticles respectively. The suffixes thnf, hnf, nf, f, s1, s2, s3 denote ternary hybrid nanofluid, hybrid nanofluid, nanofluid, base fluid, solid nanoparticles of copper (Cu), aluminum oxide (Al_2O_3), and titanium dioxide (TiO_2) correspondingly. Thermo-physical characteristics of Cu, Al_2O_3 and TiO_2 nanoparticles in pure water are presented in Table 1.

The skin friction coefficient and local Nusselt number are defined by

$$C_f Re_x^{1/2} = \frac{1}{(1-\phi_1)^{2.5}(1-\phi_2)^{2.5}(1-\phi_3)^{2.5}}f''(0) \quad \text{and} \quad Nu_x Re_x^{-1/2} = -\frac{k_{thnf}}{k_f}\theta'(0)$$

where, Re_x is the local Reynolds Number.

Table 1. Thermo-physical Properties of water and nanoparticles [2]

Physical Properties	H_2O(base fluid)	Cu (s1)	Al_2O_3 (s2)	TiO_2 (s3)
$\rho\ (kg/m^3)$	997.1	8933	3970	4250
$C_p\ (J/kgK)$	4179	385	765	686.2
$k\ (W/mK)$	0.613	401	40	8.9538
$\beta_t \times 10^5\ (K^{-1})$	21	1.67	0.85	0.9
$\sigma\ (s/m)$	5.5×10^{-6}	59.6×10^6	35×10^6	2.6×10^6

3. METHOD OF SOLUTION

The numerical solution of the non-linear higher-order system of ordinary differential equations (ODEs) given by Equations (4)-(5) and the boundary conditions (6) is performed using the bvp4c solver, which is integrated into the computational platform MATLAB. Scientists and engineers have relied heavily on this method for resolving fluid flow issues. Hale and Moore [29] pioneered the bvp4c solver, which was developed by Jacek Kierzenka and Lawrence F. Shampine of Texas's Southern Methodist University. The bvp4c solver is an approach for finite-state problems that generates fourth-order accurate numerical solutions by means of the Lobatto IIIA implicit Runge-Kutta formulation. For initial mesh point guesses and step-size modifications, this technique provides the required accuracy. According to Waini et al. [30], when compared to the shooting approach and the Keller box method, the bvp4c solver produced satisfactory results. In this context, it is necessary to decrease the derivatives of higher order with regard to η. This can be achieved by incorporating the subsequent additional variables:

$$f = y(1), \quad f' = y(2), \quad f'' = y(3), \quad \theta = y(4), \quad \theta' = y(5)$$

$$\frac{d}{d\eta}\begin{bmatrix} y(1) \\ y(2) \\ y(3) \\ y(4) \\ y(5) \end{bmatrix} = \begin{bmatrix} y(2) \\ y(3) \\ \frac{y(2)^2 - y(1)y(3) - a_2\lambda y(4) + (a_3M + a_1K)y(2) - 2a_1\gamma y(3)}{(1+2\gamma\eta)a_1} \\ y(5) \\ \frac{y(2)(y(4)+\delta) - y(1)y(5) - 2a_4\gamma y(5) - a_5 y(4)}{(1+2\gamma\eta)a_4} \end{bmatrix}$$

and boundary condition are expressed as

$$ya(1), \quad ya(2) - 1, \quad ya(4) - 1 + \delta, \quad yb(2), \quad yb(4)$$

where ya is the condition at $\eta = 0$ and yb is the condition at $\eta = \infty$

4. RESULTS AND DISCUSSION

As a comparison to the results given by Paul et al. [18], Table 2 displays the absolute values of the friction factor and the local Nusselt number as determined by the present study. We are excluding TiO_2 nanoparticle volume fractions with $Ec = 0$ from this comparison. As this research shows, the bvp4c algorithm may produce reliable numerical results that match or exceed those of competing approaches. Figs. 2-13 and Tables 2-4 illustrate the results of the computations performed numerically in the bvp4c solver of MATLAB. $Pr = 6.2, Q = 0.3, K = 1, \gamma = 0.1, Ec = 0.1, \delta = 0.3, M = 1.2, \lambda = 1.2, \phi_1 = 0.05, \phi_2 = 0.15$ and $\phi_3 = 0.2$. are the values that are employed in the study.

The thermal stratification parameter, $\delta = \frac{B}{A}$, represents the ratio of the ambient temperature gradient to the wall temperature gradient. For a physically meaningful wall heating problem, the condition $0 \leq \delta < 1$ must be satisfied so that the dimensionless wall temperature remains positive, i.e., $\theta(0) = 1 - \delta > 0$. In the present study, all numerical simulations are performed within this admissible range to ensure the physical validity of the thermal boundary conditions. As δ approaches unity, the temperature difference between the wall and the ambient fluid decreases, resulting in weaker thermal buoyancy and reduced heat transfer.

Table 2. Comparison of Skin friction Coefficient and local Nusselt Number when $\phi_3 = 0$

δ	Pr	λ	γ	Paul et al. $-C_f Re_x^{1/2}$	Present Study $-C_f Re_x^{1/2}$	Paul et al. $Nu_x Re_x^{-1/2}$	Present Study $Nu_x Re_x^{-1/2}$
0.1	6.2	1.2	0.1	2.9398	2.9795	2.7885	2.7887
0.1	2	1.2	0.1	2.8419	2.8760	1.3264	1.3311
0.1	6.2	2.4	0.1	2.7219	2.7425	2.8528	2.8516
0.1	6.2	1.2	0.2	3.0048	3.0436	2.8283	2.8269

Fig. 2 illustrates how the nanofluid's velocity $f'(\eta)$ is affected by the porosity parameter (K). As the value of the porosity parameter increases, the velocity drops. As increases, the diameter of the porous medium gradually shrinks, indicating an inverse relationship between the two variables. This smaller diameter makes the fluid's passage through the porous material more difficult. The decrease in fluid velocity was caused by the obstacle introduced by the porosity parameter (K).

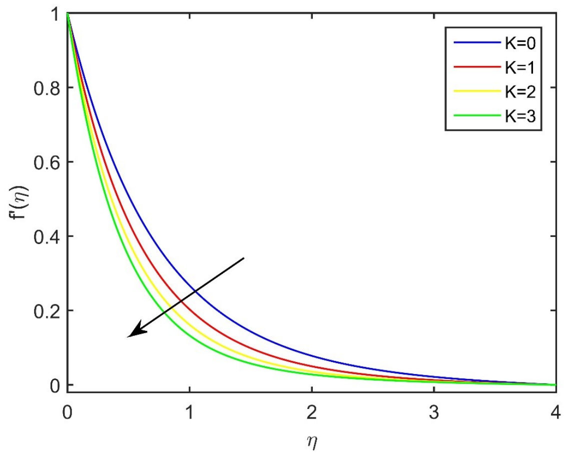

Figure 2. Effect of K on Velocity Profile

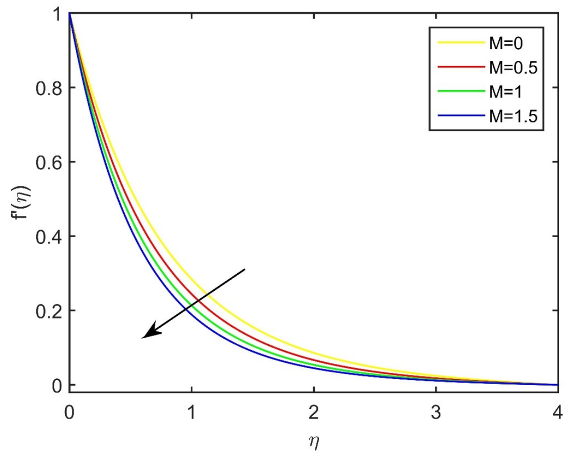

Figure 3. Effect of M on Velocity Profile

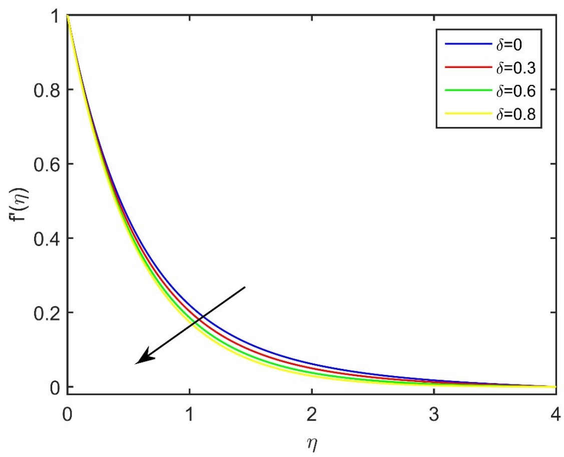

Figure 4. Effect of δ on Velocity Profile

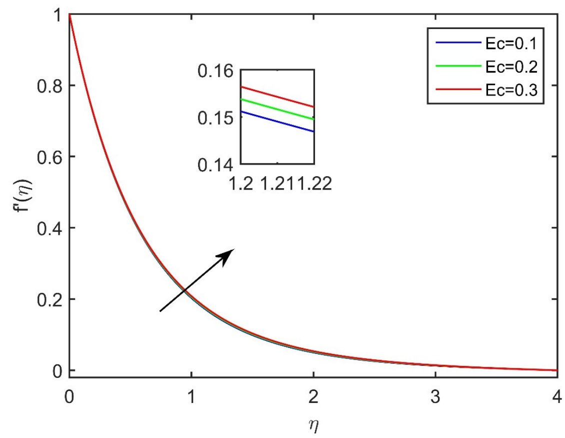

Figure 5. Effect of Ec on Velocity Profile

When the amount of M is increased, the fluid velocity drops, as portrayed in Fig. 3. Enhancing the magnetic parameter (M) causes the momentum barrier layer to become thinner. This structure develops as a consequence of the ternary hybrid nanofluid's reduced velocity caused by the Lorentz force generated by the horizontal magnetic field. Fig. 4 shows how the parameters of thermal stratification (δ) affect the nanofluid's velocity $f'(\eta)$. The flow rate drops as the heat stratification parameter rises. Reduced potent convection potential between hot wall and surrounding fluid is a result of an enhancement in the heat stratification parameter. Because of this, the buoyant force is diminished, leading to a slower flow rate.

Impact of Eckert number (Ec) on velocity profile is displayed in Fig. 5. As Ec rises velocity of the fluid also rise. Fig. 6 shows the changes in fluid velocity caused by thermal buoyancy parameter λ. We find that when values are increased, the velocity goes up. A higher increase in λ results in a stronger thermal buoyancy force. Because of this, we can deduce that buoyant forces cause the fluid's velocity to rise.

The impact of the heat source parameter (Q) is displayed in Fig. 7. It is found that fluid velocity develops in tandem with a boost in Q. Fig. 8 illustrates how the Prandtl number affects the velocity profile. The velocity profile appears to slow down as the Prandtl number increases.

The temperature profile demonstrates an enhancement as the Eckert number enhances, as illustrated in Fig. 9. The physical explanation is that an increase in Ec may cause the fluid's viscosity to absorb more energy, which it can then transform into internal energy, therefore raising the temperature. As shown in Fig. 10, the temperature $\theta(\eta)$ rises as the

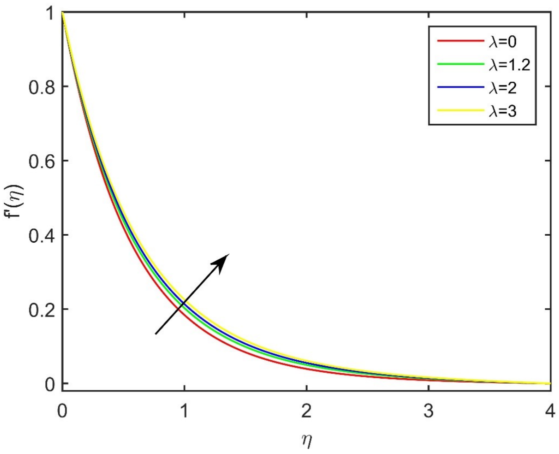

Figure 6. Effect of λ on Velocity Profile

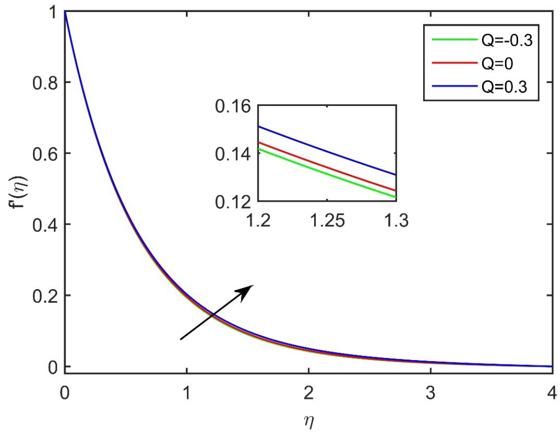

Figure 7. Effect of Q on Velocity Profile

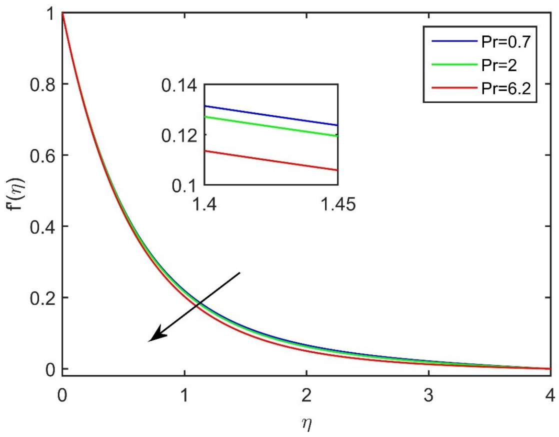

Figure 8. Effect of Pr on Velocity Profile

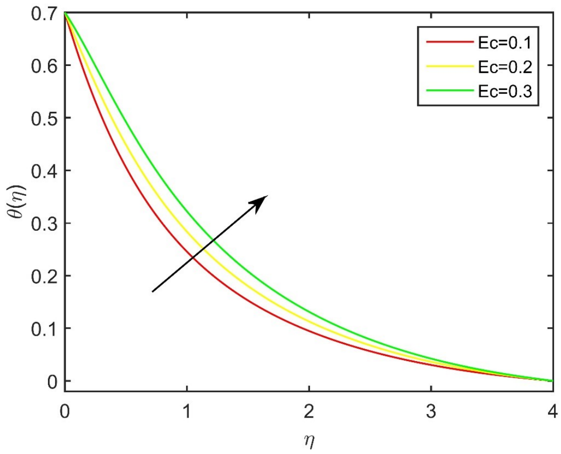

Figure 9. Effect of Ec on Temperature Profile

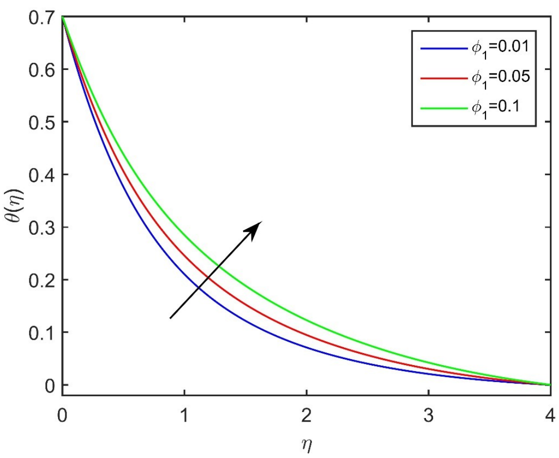

Figure 10. Effect of ϕ_1 on Temperature Profile

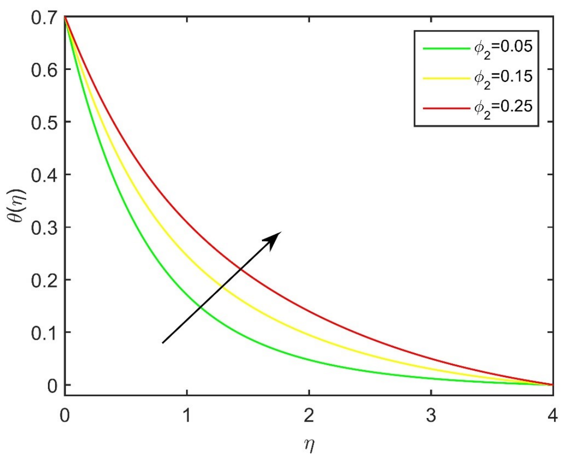

Figure 11. Effect of ϕ_2 on Temperature Profile

solid volume fraction of Cu nanoparticles grow, keeping the volume fractions of Al_2O_3 and TiO_2 constant. Moreover, it is noticeable from Fig. 11 that the temperature shows an upward trend as the volume fraction of increases, whilst the volume fractions of and stay consistent. Likewise, the temperature profile is shown to increase with an increase of ϕ_3, as depicted in Fig. 12. A higher temperature is the result of increased physical dissipation of energy, which may occur when the volume fraction of nanoparticles increases.

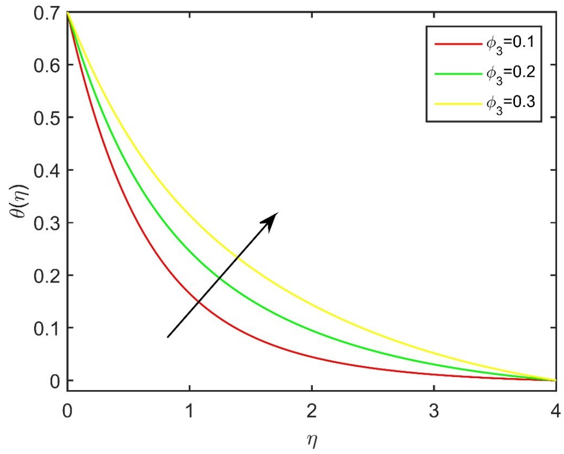

Figure 12. Effect of ϕ_3 on Temperature Profile

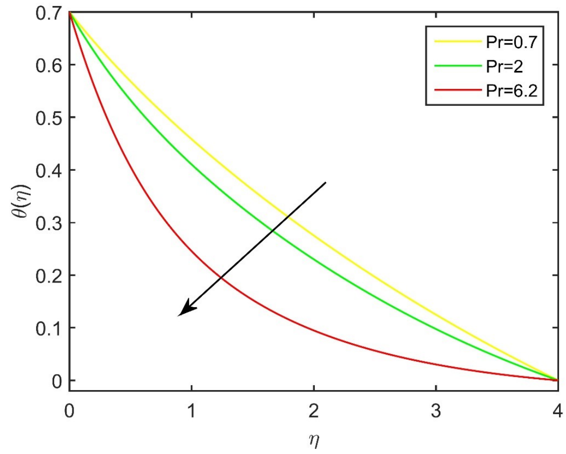

Figure 13. Effect of Pr on Temperature Profile

However, Fig. 13 highlights the consequences of the Prandtl number (Pr) on the temperature profile. Observations indicate that raising the Prandtl number results in a decline in the thickness of the heat boundary layer, resulting in a fall off in the temperature gradient. Fig. 14 demonstrates how the temperature profile is affected by a parameter of the heat source (Q). As Q, the heat source parameter, rises, the fluid temperature rises as well. This property is in accordance with the fluid's intrinsic physical properties.

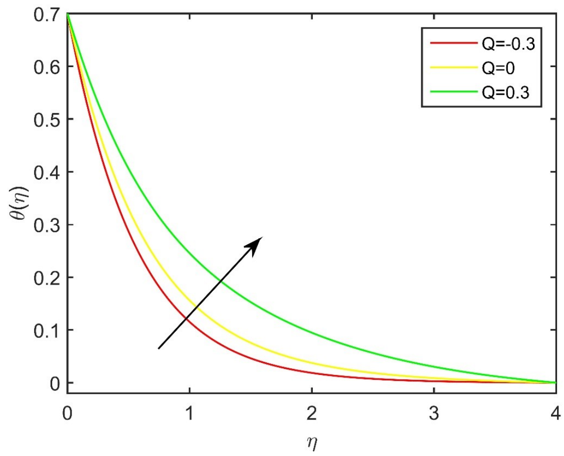

Figure 14. Effect of Q on Temperature Profile

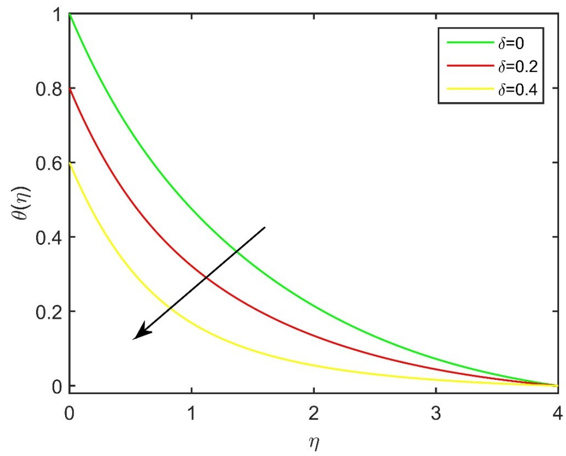

Figure 15. Effect of δ on Temperature Profile

When the temperature stratification parameter (δ) goes up, as shown in Fig. 15, the temperature of the stream goes down. When thermal stratification (δ) is present, the temperature difference between the hot wall and the fluid around it will go down. Because of this, the temperature drops and the thermal barrier layer gets thicker.

For different flow factors, Table 3 show how they change the skin friction and the local Nusselt number. Table 3 showed that the absolute value of the skin friction coefficient increases with increasing thermal stratification parameter (δ), magnetic parameter (M) and porosity parameter (K). In contrast, the local Nusselt number decreases with increasing values of δ, M, where as increases with K. For increasing λ, skin friction decreases while the local Nusselt number increases. A higher skin friction and Nusselt number are seen for Pr. As the heat source parameter (Q) increases, there is an observable decrease in the rate of heat transmission. Rising the value of the curvature parameter (γ) results in a increase in the skin friction and the Nusselt number as the value of γ increase.

In accordance with Table 4, the ternary hybrid nanofluid has a larger absolute skin friction than the hybrid nanofluid, as demonstrated by the experimental results. On the other hand, it is also noticeable that hybrid nanofluids exhibit more skin friction than ordinary nanofluids. Additionally, the ternary hybrid nanofluid has been found to demonstrate a faster rate of heat transfer than the hybrid nanofluid, which in turn shows a higher heat transfer rate than ordinary nanofluids.

Table 3. Skin friction Coefficient and Local Nusselt number for different values of $\delta, M, K, \lambda, Pr, Q, \gamma$

δ	M	K	λ	Pr	Q	γ	$-C_f Re_x^{1/2}$	$Nu_x Re_x^{-1/2}$
0							5.8976	3.3791
0.2	1.1	2	1.5	6.2	0.1	0.2	5.9937	3.1437
0.4							6.0895	2.9029
	0						5.0625	3.3897
0.2	0.5	2	1.5	6.2	0.1	0.2	5.5047	3.2716
	1.5						6.2992	3.0654
0.2	1.1	0	1.5	6.2	0.1	0.2	4.2386	2.6142
		1					5.1882	3.3559
0.2	1.1	2	1.5	6.2	0.1	0.2	6.2814	3.0258
			3				5.7207	3.2339
0.2	1.1	2	1.5	0.6	0.1	0.2	5.8739	0.9577
				4			5.9541	2.3516
0.2	1.1	2	1.5	6.2	-0.1	0.2	6.0190	3.6293
					0		6.0083	3.4083
0.2	1.1	2	1.5	6.2	0.1	0	5.7202	3.0029
						0.1	5.8582	3.0723

Table 4. Comparison of Skin friction Coefficient and Local Nusselt number

δ	Cu Nanofluid $-C_f Re_x^{1/2}$	$Cu - Al_2O_3$ Hybrid Nanofluid $-C_f Re_x^{1/2}$	$Cu - Al_2O_3 - TiO_2$ Ternary Hybrid Nanofluid $-C_f Re_x^{1/2}$	Cu Nanofluid $Nu_x Re_x^{-1/2}$	$Cu - Al_2O_3$ Hybrid Nanofluid $Nu_x Re_x^{-1/2}$	$Cu - Al_2O_3 - TiO_2$ Ternary Hybrid Nanofluid $Nu_x Re_x^{-1/2}$
0	1.9645	3.3981	5.8976	2.3250	3.0662	3.3791
0.2	2.1869	3.5020	5.9937	2.5539	2.8668	3.1437
0.5	2.3329	3.6531	6.1372	2.2778	2.5361	2.7805

5. CONCLUSIONS

An extensive study was conducted on the consequences of heating stratification and the joule's effect regarding the movement of a ternary hybrid nanofluid that demonstrates magnetohydrodynamics characteristics through a vertically stretchable cylinder. This study took into account the existence of a thermal bouncy effect and a heat source within a porous medium. The study also looks at the flow features and how they affect temperature and velocity profiles, as well as the Nusselt number and friction factor. Notable findings from this inquiry include the following:

- As the parameters δ, K, M and Pr grow, the velocity profile shows a decreasing trend, while it shows a rising pattern with higher values of λ, Ec and Q.
- With rising values of δ and Pr the temperature decline, whereas with rising values of $Ec, \phi_1, \phi_2, \phi_3$ and Q, it rises.
- Parameters δ, M, K, Q, γ and Pr cause a increase in absolute skin friction, whereas λ cause it to decrease.
- An upward trend is noted in the local Nusselt number as the values of K, Pr and λ increase, whereas a downward trend is observed as δ, M and Q increase.
- In comparison to the hybrid nanofluid, the ternary hybrid nanofluid exhibits a higher absolute skin friction. Similarly, when compared to ordinary nanofluids, hybrid nanofluids exhibit higher skin friction.
- A ternary hybrid nanofluid has a greater heat transfer rate than a hybrid nanofluid, which is also higher than that of standard nanofluids.

The present numerical investigation provides useful guidance for the design of thermal systems employing ternary hybrid nanofluids. The results indicate that moderate values of the thermal buoyancy parameter (λ) enhance the fluid velocity, while lower values of the thermal stratification parameter (δ) are preferable for maintaining higher heat transfer rates. Similarly, increasing the volume fractions of Cu, Al_2O_3 and TiO_2 nanoparticles improves the thermal performance of the base fluid, although excessively high nanoparticle concentrations may increase skin friction and pumping power requirements. The magnetic parameter (M) and porosity parameter (K) should therefore be selected carefully to achieve an appropriate balance between flow resistance and heat transfer enhancement. These findings suggest that the $Cu - Al_2O_3 - TiO_2/H_2O$ ternary hybrid nanofluid can be effectively utilized in geothermal heat extraction, compact heat exchangers, solar thermal collectors, electronic cooling systems, and chemical processing equipment where efficient thermal management is required.

ORCID

Surajit Dutta, https://orcid.org/0009-0008-7188-3919; **Nitul Kalita**, https://orcid.org/0000-0001-8348-2225; **Rupam Shankar Nath**, https://orcid.org/0009-0002-2352-0538; **Rudra Kanta Deka**, https://orcid.org/0009-0007-1573-4890

REFERENCES

[1] S.U.S. Choi, and J.A. Eastman, "Enhancing thermal conductivity of fluids with nanoparticles," Technical report, Argonne National Lab. (ANL), Argonne, IL (United States), 1995.

[2] S. Das, and R.N. Jana, "Natural convective magneto-nanofluid flow and radiative heat transfer past a moving vertical plate," Alexandria Engineering Journal, **54**(1), 55–64 (2015). https://doi.org/10.1016/j.aej.2015.01.001

[3] S. Das, R.N. Jana, and O.D. Makinde, "Transient natural convection in a vertical channel filled with nanofluids in the presence of thermal radiation," Alexandria Engineering Journal, **55**(1), 253–262 (2016). https://doi.org/10.1016/j.aej.2015.10.013

[4] P.C. Reddy, M.C. Raju, and G.S.S. Raju, "Free convective heat and mass transfer flow of heat-generating nanofluid past a vertical moving porous plate in a conducting field," Special Topics & Reviews in Porous Media: An International Journal, **7**(2), (2016). https://doi.org/10.1615/specialtopicsrevporousmedia.2016016973

[5] B. Mahanthesh, B.J. Gireesha, and R.S.R. Gorla, "Heat and mass transfer effects on the mixed convective flow of chemically reacting nanofluid past a moving/stationary vertical plate," Alexandria engineering journal, **55**(1), 569–581 (2016). https://doi.org/10.1016/j.aej.2016.01.022

[6] N. Sandeep, and M.G. Reddy, "Heat transfer of nonlinear radiative magnetohydrodynamic cu-water nanofluid flow over two different geometries," Journal of Molecular Liquids, **225**, 87–94 (2017). https://doi.org/10.1016/j.molliq.2016.11.026

[7] M. Sheikholeslami, M.G. Bandpy, R. Ellahi, and A. Zeeshan, "Simulation of MHD CuO–water nanofluid flow and convective heat transfer considering Lorentz forces," Journal of Magnetism and Magnetic Materials, **369**, 69–80 (2014). https://doi.org/10.1016/j.jmmm.2014.06.017

[8] M.M. Rashidi, E. Momoniat, M. Ferdows, and A. Basiriparsa, "Lie group solution for free convective flow of a nanofluid past a chemically reacting horizontal plate in a porous media," Mathematical Problems in Engineering, **2014**, (2014). http://dx.doi.org/10.1155/2014/239082

[9] M.H. Abolbashari, N. Freidoonimehr, F. Nazari, and M.M. Rashidi, "Entropy analysis for an unsteady MHD flow past a stretching permeable surface in nano-fluid," Powder Technology, **267**, 256–267 (2014). https://doi.org/10.1016/j.powtec.2014.07.028

[10] M. Turkyilmazoglu, "Exact analytical solutions for heat and mass transfer of MHD slip flow in nanofluids," Chemical Engineering Science, **84**, 182–187 (2012). https://doi.org/10.1016/j.ces.2012.08.029

[11] T.G. Motsumi, and O.D. Makinde, "Effects of thermal radiation and viscous dissipation on boundary layer flow of nanofluids over a permeable moving flat plate," Physica Scripta, **86**(4), 045003 (2012). https://doi.org/10.1088/0031-8949/86/04/045003

[12] R.S. Nath, and R.K. Deka, "The effects of thermal stratification on flow past an infinite vertical plate in presence of chemical reaction," East European Journal of Physics, (3), 223–232 (2023). https://doi.org/10.26565/2312-4334-2023-3-19

[13] N. Kalita, R.K. Deka, and R.S. Nath, "Unsteady flow past an accelerated vertical plate with variable temperature in presence of thermal stratification and chemical reaction," East European Journal of Physics, (3), 441–450 (2023). https://doi.org/10.26565/2312-4334-2023-3-49

[14] R.S. Nath, R.K. Deka, and H. Kumar, "The effect of thermal stratification on unsteady parabolic flow past an infinite vertical plate with chemical reaction," East European Journal of Physics, (4), 77–86 (2023). https://doi.org/10.26565/2312-4334-2023-4-08

[15] C.-Y. Cheng, "Double-diffusive natural convection along a vertical wavy truncated cone in non-newtonian fluid saturated porous media with thermal and mass stratification," International Communications in Heat and Mass Transfer, **35**(8), 985–990 (2008). https://doi.org/10.1016/j.icheatmasstransfer.2008.04.007

[16] C.-Y. Cheng, "Combined heat and mass transfer in natural convection flow from a vertical wavy surface in a power-law fluid saturated porous medium with thermal and mass stratification," International Communications in Heat and Mass Transfer, **36**(4), 351–356 (2009). https://doi.org/10.1016/j.icheatmasstransfer.2009.01.003

[17] A. Paul, R.K. Deka, et al. "Unsteady natural convection flow past an infinite cylinder with thermal and mass stratification," Int. J. Eng. Math, **2017**, 8410691 (2017). https://doi.org/10.1155/2017/8410691

[18] A. Paul, J.M. Nath, and T.K. Das, "An investigation of the MHD Cu-Al_2O_3/H_2O hybrid-nanofluid in a porous medium across a vertically stretching cylinder incorporating thermal stratification impact," Journal of Thermal Engineering, **9**(3), 799-810 (2023). https://doi.org/10.18186/thermal.1300847

[19] P. Rana, and A. Kumar, "Nonlinear buoyancy driven flow of hybrid nanoliquid past a spinning cylinder with quadratic thermal radiation," International Communications in Heat and Mass Transfer, **139**, 106439 (2022). https://doi.org/10.1016/j.icheatmasstransfer.2022.106439

[20] M. Shanmugapriya, R. Sundareswaran, P.S. Kumar, and G. Rangasamy, "Impact of nanoparticle shape in enhancing heat transfer of magnetized ternary hybrid nanofluid," Sustainable Energy Technologies and Assessments, **53**, 102700 (2022). https://doi.org/10.1016/j.seta.2022.102700

[21] J. Shaik, B.A.R. Polu, M.M. Ahmed, and R.A. Mohamed, "Characteristics of moving hot block and non-fourier heat flux model on sinusoidal wavy cavity filled with hybrid nanofluid," The European Physical Journal Plus, **137**(1), 131 (2022). https://doi.org/10.1140/epjp/s13360-022-02361-y

[22] W. Cao, I.L. Animasaun, S.-J. Yook, V.A. Oladipupo, and X. Ji, "Simulation of the dynamics of colloidal mixture of water with various nanoparticles at different levels of partial slip: Ternary-hybrid nanofluid," International Communications in Heat and Mass Transfer, **135**, 106069 (2022). https://doi.org/10.1016/j.icheatmasstransfer.2022.106069

[23] S. Nasir, S. Sirisubtawee, P. Juntharee, A.S. Berrouk, S. Mukhtar, and T. Gul, "Heat transport study of ternary hybrid nanofluid flow under magnetic dipole together with nonlinear thermal radiation," Applied Nanoscience, **12**(9), 2777–2788 (2022). https://doi.org/10.1007/s13204-022-02583-7

[24] Z. Mahmood, Z. Iqbal, M.A. Alyami, B. Alqahtani, M.F. Yassen, and U. Khan, "Influence of suction and heat source on mhd stagnation point flow of ternary hybrid nanofluid over convectively heated stretching/shrinking cylinder," Advances in Mechanical Engineering, **14**(9), 16878132221126278 (2022). https://doi.org/10.1177/16878132221126278

[25] S. Jakeer, S.R.R. Reddy, A.M. Rashad, M.L. Rupa, and C. Manjula, "Nonlinear analysis of Darcy-Forchheimer flow in EMHD ternary hybrid nanofluid (Cu-CNT-Ti/water) with radiation effect," Forces in Mechanics, **10**, 100177 (2023). https://doi.org/10.1016/j.finmec.2023.100177

[26] P.M. Patil, B. Goudar, and M.A. Sheremet, "Tangent hyperbolic ternary hybrid nanofluid flow over a rough-yawed cylinder due to impulsive motion," Journal of Taibah University for Science, **17**(1), 2199664 (2023). https://doi.org/10.1080/16583655.2023.2199664

[27] E.H. Gorfie, A.T. Moltot, G.A. Zergaw, and H. Dessie, "Influence of joule heating and nonlinear thermal radiation on the electrical conductivity of second-grade hybrid nanofluid flow over a stretching cylinder," Engineering Reports, **7**(4), e70129 (2025). https://doi.org/10.1002/eng2.70129

[28] P. Kumar, R.S. Yadav, and O.D. Makinde, "Numerical study of Williamson fluid flow and heat transfer over a permeable stretching cylinder with the effects of joule heating and heat generation/absorption," Heat Transfer, **52**(4), 3372–3388 (2023). https://doi.org/10.1002/htj.22832

[29] N.P. Hale, M.Sc. Thesis, "A sixth-order extension to the MATLAB bvp4c software of J. Kierzenka and L. Shampine." Department of Mathematics, Imperial College London, 2006.

[30] I. Waini, A. Ishak, and I. Pop, "Mixed convection flow over an exponentially stretching/shrinking vertical surface in a hybrid nanofluid," Alexandria Engineering Journal, **59**(3), 1881–1891 (2020). https://doi.org/10.1016/j.aej.2020.05.030

ВПЛИВ ЕФЕКТУ ДЖОУЛЕВОГО НАГРІВАННЯ ТА ТЕПЛОВОГО РОЗШИРЕННЯ НА МГД-ПОТРІЙНУ ГІБРИДНУ НАНОРІДИНУ В ПОРИСТОМУ СЕРЕДОВИЩІ НАД ВЕРТИКАЛЬНО РОЗТЯГНУТИМ ЦИЛІНДРОМ: ЧИСЛОВЕ ДОСЛІДЖЕННЯ

Сураджіт Дутта[1], Нітул Каліта[2], Рупам Шанкар Натх[3], Рудра Канта Дека[2]

[1]*Кафедра математики, C.N.B. Коледж, Бокахат-785612, Ассам, Індія*

[2]*Кафедра математики, Університет Гаухаті, Гувахаті-781014, Ассам, Індія*

[3]*Кафедра математики, Коледж Морігаон (Автономний), Морігаон-782105, Ассам, Індія*

У цьому дослідженні чисельно досліджено аспекти потоку в магнітогідродинамічній (МГД) потрійній гібридній нанорідині, що складається з суспендованих наночастинок (Cu), оксиду алюмінію (Al_2O_3) та діоксиду титану (TiO_2) у воді (H_2O). Вплив термічної стратифікації та джоулевого нагрівання враховується шляхом пропускання нанорідини через вертикально простягаючийся циліндр у пористому середовищі. Шляхом реалізації відповідного перетворення, рівняння енергії та пограничного шару спрощуються до нелінійної системи звичайних диференціальних рівнянь (ЗДР). Отримана система розв'язується за допомогою розв'язувача bvp4c четвертого порядку точності MATLAB. Для розв'язання зміненої системи використовується MATLAB. Ефекти графічно проілюстровано зміною швидкості та температури, а також кількісно представлено в таблиці зміни коефіцієнта тертя та швидкості теплопередачі для важливих значень безрозмірних фізичних факторів, пов'язаних з проблемою. Важливі результати показують, що гібридні нанорідини перевершують нанорідини з точки зору теплопровідності. Температура та швидкість потрійної гібридної нанорідини зменшуються при наявності коефіцієнта теплової стратифікації порівняно з відсутністю стратифікації. Спостерігається помітне збільшення швидкості теплопередачі при порівнянні потрійної гібридної нанорідини з гібридною нанорідиною, що, у свою чергу, перевершує показники традиційних нанорідин. Отримані результати є цінними для застосування у видобутку геотермальної енергії, хімічній обробці та синтезі матеріалів.

Ключові слова: *потрійна гібридна нанорідина; ефект Джоуля; розтягування вертикального циліндра; термічна стратифікація; пористе середовище; bvp4c*